

Article

# Supply and Demand Forecasting-Based Optimal Energy Sharing Strategies for Grid-Integrated Community Networks

Adugna Gebrie Jember<sup>1</sup>, Ruiyu Bao<sup>1</sup>, Zijia Yao<sup>1</sup>, Zhao Wang<sup>1,\*</sup>, Zhenyu Zhou<sup>1</sup> and Xiaoyan Wang<sup>2</sup>

<sup>1</sup> Key Laboratory of Alternate Electrical Power System with Renewable Energy Sources, North China Electric Power University, Beijing 102206, China

<sup>2</sup> Graduate School of Science and Engineering, Ibaraki University, Ibaraki 310-8512, Japan

\* Correspondence: zhaow@ncepu.edu.cn

Received: 23 July 2024; Revised: 17 October 2024; Accepted: 17 October 2024; Published: 5 November 2024

**Abstract:** This research introduces a model with two distinct stages for accurate forecasting and efficient energy sharing within grid-integrated community networks (GICNs), which combines residential power loads, generators of wind and photovoltaic (PV) power, and energy storage (ES). In the first-stage system model, we employ a machine learning (ML) algorithm for day-ahead supply and demand forecasting to improve the forecasting accuracy. Specifically, we develop a hybrid convolutional neural network with long short-term memory (CNN-LSTM), which effectively includes both spatial and temporal dimensions of time series data. In the second stage, a bidirectional real-time energy sharing strategy is designed based on forecasted data, facilitating the efficient distribution of surplus energy among communities. The two-stage system model integrates forecasting and energy sharing to accurately predict supply and demand, as well as effective energy sharing among GICN participants. The measurements including mean absolute error (MAE), root mean squared error (RMSE), and generation utilization rate are defined to evaluate prediction accuracy and energy sharing effectiveness thereby ensuring optimal grid operation and sustainability. Finally, the proposed hybrid CNN-LSTM algorithm is compared with the single LSTM and CNN models to demonstrate the performance superiority of the hybrid CNN-LSTM model. Numerical simulation experiments indicate that the proposed model CNN-LSTM achieved high accuracy in predicting user PV, wind, and load demand. Additionally, the implemented real-time energy sharing strategy efficiently manages energy distribution within GICNs.

**Keywords:** supply and demand forecasting; energy sharing; convolutional neural network with long short-term memory (CNN-LSTM) networks; grid-integrated networks; self-sufficiency ratio (SSR); self-consumption rate (SCR)

## 1. Introduction

In the growing landscape of energy management, the integration of renewable energy sources and smart grid technologies has revolutionized the landscape of modern energy systems, offering unique opportunities for sustainability and efficiency. The transition to renewable energy sources in grid-integrated systems is a critical step in achieving sustainability and resilience in energy supply [1–3]. With the application of renewable energy sources such as wind and PV power generation, the energy management landscape is undergoing a significant transformation. However, these renewable energy sources have inconsistency and uncertainty in energy supply, challenging smart energy management and distribution systems. To address these challenges, advanced energy management strategies are being developed, focusing on optimizing the integration of wind and PV generation with active distribution network (ADN) [4–6].

Grid-integrated community networks (GICNs) represent a novel paradigm in the developing grid-integrated network and offer a promising framework for improving energy efficiency, reliability, and sustainability. These networks are geographically formed as clusters of neighboring consumers and producers (prosumers) of energy, integrated into the ADN, and capable of localized energy exchange. By leveraging local renewable energy sources and enabling energy sharing strategies among community members, GICNs can maintain a balance between supply and demand within the community [7–9]. An effective energy sharing strategy can dynamically match energy supply from PV and wind generation and energy storage (ES) systems with the demand profiles of



community members. This approach minimizes reliance on the traditional grid and reduces overall energy costs and energy wastage [10–12].

The key to optimizing energy sharing strategies lies in accurate supply and demand forecasting. Accurately forecasting the availability of wind and PV generation, local load, and ES status is an important factor and it is a complex task for enabling effective real-time energy sharing and improving the sustainability of power systems within GICNs [13]. Machine learning (ML) techniques have emerged as powerful tools for addressing the key challenges in accurate supply and demand forecasting, providing effective solutions by analyzing large amounts of historical data to predict future outcomes [14–16]. ML algorithms including convolutional neural networks (CNNs), and long short-term memory (LSTM) networks are nowadays used to predict both energy supply and load demands. CNN and LSTM networks are effective prediction algorithms in ML, and they are each suited for specific aspects of forecasting supply and demand. CNN is adept at processing spatial data feature extraction due to its ability to detect patterns and structures in multidimensional inputs from large and complex datasets. LSTM is mostly effective in handling time series data and capturing long-term temporal dependencies [17–19]. However, the supply and demand forecasting-based energy sharing strategies for GICNs still face the following challenges:

- (1) Develop an ML model for accurate supply and demand forecasting: Due to the distinct spatial and temporal characteristics of supply and demand in GICNs, using CNN and LSTM algorithms separately for forecasting poses challenges. CNN is adept at learning spatial hierarchies from multidimensional time series data but struggles with capturing long-term temporal dependencies. While LSTM is effective in sequence dependency but struggles with spatial feature extraction.
- (2) Imbalance between supply and demand: Accurately forecasting the user's PV and wind generations as well as load demand in order to achieve accurate energy demand in real-time is a critical challenge that affects the energy balance and optimal energy sharing decision. Due to different PV and wind energy patterns and demand fluctuation throughout different time periods, different degrees of energy imbalance will happen in different GICNs, which increases the complexity of the supply and demand forecasting and the energy sharing strategy that needs to be addressed.
- (3) Optimal real-time energy sharing strategies: Developing optimal energy sharing strategies for GICNs presents a unique challenge. These strategies must dynamically adapt energy generation, consumption, and storage among users in real-time to maximize renewable energy sources utilization efficiency and minimize energy purchase and energy wastage. Real-time optimization algorithms need to account for the dynamic nature of energy scheduling and sharing.

Nowadays, numerous studies have addressed energy sharing strategies and supply and demand forecasting. In [14], A. Golder et al. proposed the use of ML algorithm models to improve the forecasting accuracy for electricity demand and PV generation. The authors evaluated three models, i.e., support vector machines (SVM), multi-layer Perceptron (MLP), and LSTM models individually. However, the study focused on improving forecasting accuracy but did not fully explore the potential of hybrid ML algorithms, nor did it consider the relationship between accurate forecasting systems and real-time energy sharing strategies. In [17], L. Wen et al. proposed aggregated load and PV generation forecasting to achieve optimal load dispatching for community microgrids using deep recurrent neural network with an LSTM model. However, the study focused on LSTM model, which may limit forecasting accuracy. The optimization approach did not fully address forecasting-based real-time energy sharing strategies, which are essential for adapting to sudden changes in power supply and demand. In [18], F. Qayyum et al. proposed a forecasting optimization model for minimizing energy costs and improving energy sharing in peer-to-peer (P2P) nano-grid systems. The study introduced a two-stage approach which uses bidirectional-LSTM for energy load and PV generation forecasting and develops an energy sharing strategy that defines the roles of nano-grids as prosumers by using a particle swarm optimization (PSO) algorithm. However, the study focused on single ML algorithm and neglected to consider hybrid ML algorithms that combine the strengths of different models to improve forecasting accuracy.

In order to solve the above-mentioned challenges, we design a two-stage system model for accurately forecasting and efficient energy sharing of GICNs, which combines ML-based supply and demand forecasting and a bidirectional real-time energy sharing strategy. Unlike previous studies that focus on either spatial or temporal methods independently, this paper proposes a hybrid CNN-LSTM model. By combining the strengths of the individual models, the hybrid CNN-LSTM model leverages both spatial and temporal information, allowing more accurate forecasting of energy supply and demand. This accuracy is crucial for improving energy-sharing strategies within GICNs, leading to more efficient energy sharing strategies. Compared to individual CNN or LSTM models, the hybrid CNN-LSTM model approach outperforms in terms of both forecasting accuracy and

computational efficiency, addressing the limitations of using either model alone. The main contributions of this paper are summarized as follows.

- (1) Design the two-stage system model and implementation procedure: We design the two-stage system model and implementation method for accurate prediction and efficient energy sharing of GICNs which includes residential power load, generations for wind and PV power, and ES.
- (2) Propose the first-stage system model based on hybrid CNN-LSTM: We propose the first-stage system model as the day-ahead supply and demand forecasting model to predict PV and wind as well as load demand in order to achieve accurate predictions. Specifically, we develop hybrid CNN-LSTM models which are mostly effective for tasks to understand both the spatial and temporal dimensions of the time series data.
- (3) Propose the second-stage system model as energy sharing system strategies: We propose the second-stage system model as a bidirectional real-time energy sharing based on the forecasted data to dynamically facilitate the efficient distribution of surplus energy among GICNs. The system aims to accurately represent the interaction among GICNs and power utilities (ADN) ensuring efficient energy sharing. The real-time energy sharing optimization algorithms account for the dynamic nature of energy sharing to maximize renewable energy resource utilization and minimize the cost of energy bought.

## **2. Related Works**

To address the challenges mentioned above, it is essential to review relevant and recent existing research and solutions. In [12], N. Liu et al. proposed an online energy sharing method for nano-grid power systems to improve self-sufficiency and PV consumption. The method introduced a hybrid P2P energy sharing framework that combines P2P physical systems with a cyber system. To address the stochastic nature of PV and user load, the authors developed an online optimization model based on Lyapunov optimization, aiming to maximize self-sufficiency. However, the study focused on the optimal energy sharing strategies without considering real-time supply and demand forecasting techniques for nano-grid power systems. In [19], K. Wang et al. proposed a hybrid deep learning model combining LSTM and CNN for PV power forecasting. This model addresses the challenges posed by the intermittent nature of PV by first extracting temporal features using LSTM and then spatial features using CNN. The study compared the performance of hybrid model with that of single models. However, this study did not fully consider a two-stage system model that combines accurate supply-demand forecasting with optimal real-time energy sharing. In [20], X. Zhang et al. proposed an optimal energy dispatch method for grid-integrated 5G base stations (BSs). The study addressed the uncertainty caused by the wide distribution, small volume, and large load fluctuations of PV-integrated 5G BSs when directly participating in demand response (DR). The method used contract theory to incentivize participation in peak-shaving for the grid side and proposed a Lyapunov-based algorithm to optimize energy sharing among the BSs, improving PV usage and stabilizing the ES. However, the study focused on predefined timescales for DR planning and energy sharing optimization without considering real-time forecasting techniques for energy demand and supply. In [21], M. Shi et al. developed a short-term PV power forecasting model using a LSTM network. The study emphasized the importance of accurate PV power forecasting due to the inherent randomness and fluctuations in PV output. Pearson correlation analysis was used to identify features that significantly influence PV power. However, the study primarily focused on using single LSTM algorithm without considering the potential benefits of hybrid forecasting approaches that could integrate multiple ML techniques to further improve forecasting accuracy.

The abovementioned studies often focus on one aspect without fully considering the relationship between accurate supply and demand forecasting using hybrid ML algorithms with real-time energy sharing strategies. Our approach bridges this gap by integrating both supply and demand forecasting techniques and real time energy sharing strategies as a two-stage system model. This integration is essential because accurate forecasting directly influences the efficiency of energy sharing in real time scenarios. By addressing both aspects simultaneously, the two-stage system model approach is advanced in terms of both supply and demand forecasting accuracy using hybrid ML algorithms and energy sharing efficiency, ultimately leading to more sustainable and cost-effective GICN operation. Through this forecasting-based optimal energy sharing framework, we contribute to advancing the integration and management of renewable energy sources in GICNs, paving the way for more resilient and sustainable energy infrastructures.

## **3. System Model and Implementation Procedure**

In this section, we design a two-stage system model and implementation method for accurate forecasting and efficient energy sharing of GICNs, as shown in Figure 1. In the first-stage system model, we propose a hybrid CNN-LSTM-based day-ahead supply and demand forecasting method to predict PV and wind output power as well as load demand to balance supply and demand among GICNs. Additionally, the system incorporates an energy

sharing strategy as the second-stage system model to achieve efficient energy sharing and energy utilization and remit supply-demand imbalances among community participants. The implementation procedure involves several steps to develop, train, and deploy the forecasting and energy sharing optimization models within the system as follows.

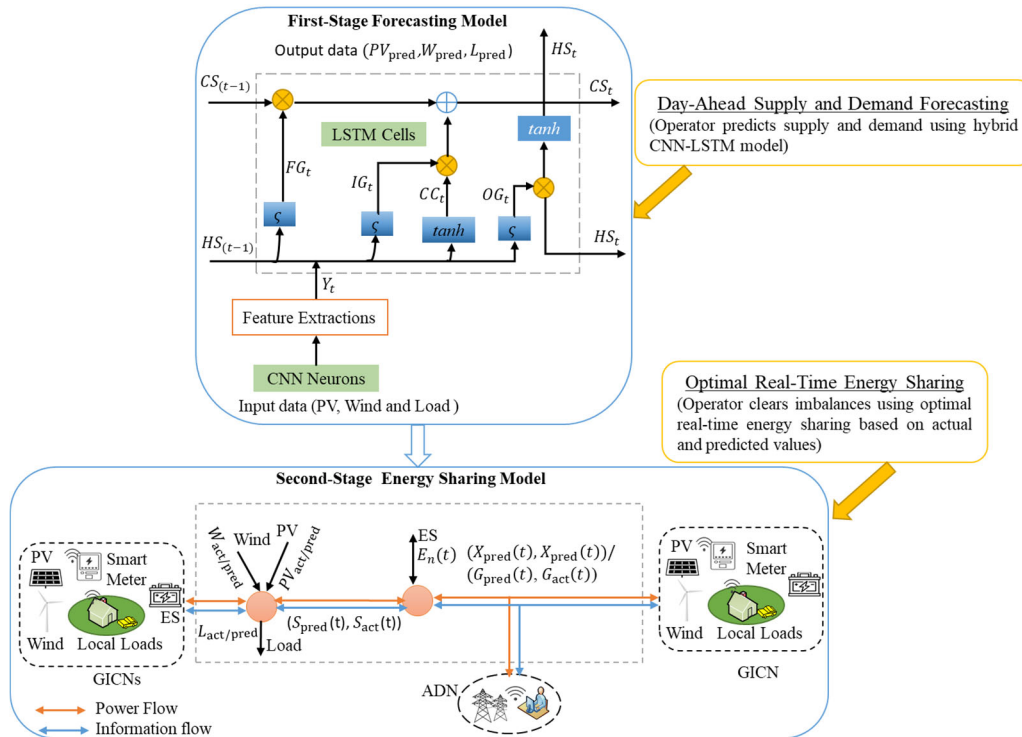


**Figure 1.** Two-stage system model (day-ahead hybrid CNN-LSTM-based supply and demand forecasting and bidirectional real-time energy sharing).

- (1) Data collection and preprocessing: First, historical data of GICN users are gathered (PV, wind, and load demand). Data preprocessing techniques are applied to clean the data, handle missing values, and normalize the data for model training. The transformation from the original values to the scaled values often involves normalization techniques using the common approach of Min-Max scaling (normalization), which linearly transforms the data to a default range of  $[0,1]$ . Given an original value  $y$ , the scaled value  $y'$  is computed as  $y' = \frac{y - y_{\min}}{y_{\max} - y_{\min}}$ .  $y'$  is the scaled values.  $y_{\max}$  and  $y_{\min}$  are the maximum and minimum values in the dataset. The scaled value  $y'$  falls within the range  $[0,1]$  [17].
- (2) Forecasting model development using CNN-LSTM: The hybrid CNN-LSTM model approach combines CNN's ability to extract spatial features from data with LSTM's ability to capture long-term dependencies. The combination of CNN-LSTM is mostly suited for forecasting tasks where both spatial patterns and temporal sequences are pivotal for accurate predictions. CNN-LSTM is implemented to develop forecasting models for GICN users' supply and demand using Python libraries such as the PyTorch. Model parameters, including the number of layers, the size of the convolutional filters, hidden units, sequence length, and the number of CNN-LSTM units, are fine-tuned through a series of experiments to optimize performance.
- (3) Energy sharing model: After the first-stage system model is completed, we design a second-stage system model as a real-time energy sharing strategy to dynamically facilitate the efficient distribution of surplus energy. The model utilizes forecasted energy generation and load demand to optimize energy sharing among GICN users.
- (4) Performance evaluation and monitoring: For the first-stage system model, the performance metrics for the forecasting models evaluate the effectiveness of our CNN-LSTM model, mostly using mean absolute error (MAE) and root mean squared error (RMSE) metrics. We conduct a series of tests to compare the forecasting accuracy of CNN-LSTM with that of a single LSTM and CNN model. For the second-stage

system model, the performance evaluations of the real-time energy sharing strategies include energy efficiency, generation utilization rates, self-sufficiency, and self-consumption ratio.

#### 4. First-Stage CNN-LSTM-Based Forecasting Model

In this section, we design a hybrid CNN-LSTM-based forecasting structure as the first-stage system model. This design combines the strengths of CNN and LSTM networks to analyze time series data for tasks that require understanding spatial features and long-term temporal dependencies. As shown in Figure 2, CNNs are first adopted to learn spatial hierarchies of features from input (PV, wind, and load) time series data. Through the usage of filters/kernels, CNN can efficiently process data with high dimensionality, making it highly effective for tasks involving multi-dimensional time series data [22]. LSTM is a special kind of recurrent neural network (RNN). It is designed to avoid the long-term dependency problem, making the input data suitable for tasks requiring the understanding of relationships and patterns over long sequences and handling time series data forecasting [18]. While CNN is adept at learning spatial hierarchies from multidimensional time series data, it is not effective at capturing long-term temporal dependencies. LSTM is effective in sequence dependency but struggles with spatial feature extraction. Therefore, we develop a hybrid CNN-LSTM model to address the challenges that either CNN or LSTM might face when individually handling complex forecasting tasks. By combining these two powerful neural network algorithms, the CNN-LSTM model leverages improved performance for forecasting PV and wind as well as load demand involving time series data with spatial and temporal dynamics. The hybrid model uses CNN for efficient spatial feature extraction before these features are processed by LSTM for temporal analysis.

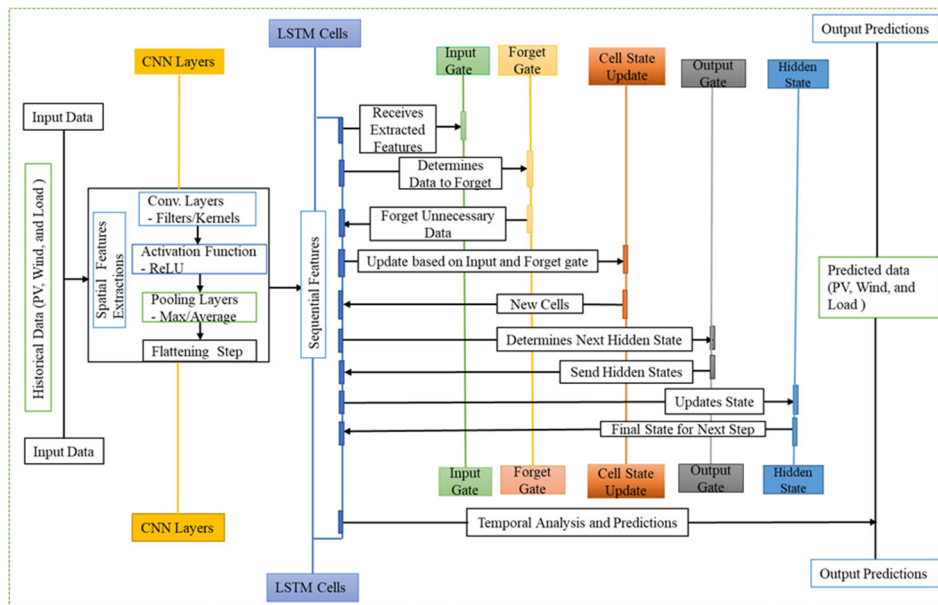


**Figure 2.** Sequence structure flow of the first-stage hybrid CNN-LSTM-based forecasting model.

In Figure 2, the spatial feature extraction steps are performed by the CNN layers. Convolutional layers are used as filter/kernels to perform convolution operations on the input. Activation functions are put on Rectified Linear Unit (ReLU) to incorporate functions that allow the network to capture and model complex features that are not simply linear relationships. Pooling layers are used to perform downsampling operations as max/average to decrease the spatial dimensions of data. The flattening step is used to flatten data into a single vector, which usually occurs before passing the features to the LSTM layers in the hybrid model. These CNN steps are used as the sequence input for the subsequent LSTM layers to capture temporal or sequence dependencies for processing and prediction. LSTM is particularly adept at processing these features to recognize patterns over time or sequence, which is difficult to capture with a CNN alone. This step emphasizes the transition from spatial feature extraction to preparing the data for temporal analysis by highlighting that the extracted features are sequential, making them suitable for time-series analysis and temporal context. The internal structural design for each LSTM cell unit, or memory cell, contains three control gates, i.e., input, output, and forget, as shown in Figures 1 and 2. These gates control the data flow information within the cell and help in controlling memory preservation and utilization.

#### 4.1. Model Operation Formulations

In our proposed hybrid model, the CNN component first processes data input including the PV and wind generation as well as the load demand to extract features and reduce data complexity. Then, these extracted features are fed into an LSTM network as sequential input to learn the temporal or sequential relationships in the data. It performs its complex gate-regulated operations to update its internal state and produce an output [18]. The LSTM cell's network flow equations are given by

$$IG_t = \zeta(W_{IG} \cdot [HS_{t-1}, Y_t] + B_{IG}) \quad (1)$$

$$FG_t = \zeta(W_{FG} \cdot [HS_{t-1}, Y_t] + B_{FG}) \quad (2)$$

$$CS_t = FG_t \cdot CS_t + IG_t \cdot CC_t \quad (3)$$

$$CC_t = \tanh(W_{CS} \cdot [HS_{t-1}, Y_t] + B_{CS}) \quad (4)$$

$$OG_t = \zeta(W_{OG} \cdot [HS_{t-1}, Y_t] + B_{OG}) \quad (5)$$

$$HS_t = OG_t \cdot \tanh(CS_t) \quad (6)$$

where  $t=1:T$ ,  $t$  is the time step index, and  $T$  is the total number of time steps over dataset points.  $Y_t$  represents the current input data.  $IG_t$ ,  $FG_t$ , and  $OG_t$  are the control gates of input, output, and forget at time step  $t$ .  $W_{IG}$ ,  $W_{FG}$ ,  $W_{OG}$ , and  $W_{CS}$  are the weight matrices for each gate and cell state.  $B_{IG}$ ,  $B_{FG}$ ,  $B_{CS}$ , and  $B_{OG}$  are the biased terms.  $CS_t$ ,  $CC_t$ , and  $HS_t$  are the cell, candidate, and hidden states.  $\zeta$  and  $\tanh$  are the activation function in the network.  $FG_t$  decides what information the LSTM should remove from the  $CS_t$ . It takes the previous  $HS_{t-1}$  and the current  $Y_t$  and applies a sigmoid function to each number in those vectors to produce a value between 0 and 1. These values are then multiplied by the  $CS_t$ . A value close to 0 means forgetting this information while a value close to 1 means retaining this information. Similarly,  $IG_t$  decides which values in the cell state to update,  $CC_t$  is a vector of new values that could be added to the cell state. Then,  $CS_t$  combines old cell state and new candidate values to form the new cell state, considering what to forget and what to add.  $OG_t$  decides what the next hidden state should be based on the cell state and allows only certain parts to affect the output.  $HS_t$  is the output of the LSTM unit and is used for prediction and passed to the next time step [19]. This network flow allows LSTMs to make selective decisions about what data to store, remove, and output at each step in a sequence to handle long-range dependencies in data effectively.

These formulas define how information flows through the LSTM cells after the CNN is processed and how the hidden states are updated over time. The model parameters (weights and biases) are learned during the training process to minimize the prediction error. In the Adam optimizer formula, the updated parameter values at time step  $t$  are given by

$$\theta_{t+1} = \theta_t - \frac{\eta}{\sqrt{\hat{v}_t} + \epsilon} \cdot \hat{m}_t \quad (7)$$

where  $\theta_{t+1}$  is the updated values at time step  $t+1$  and  $\theta_t$  is the current values at time step  $t$ .  $\eta$  is the learning rate, which controls the step size during parameter updates.  $\hat{v}_t$  and  $\hat{m}_t$  are bias-corrected versions of the first and second-moment estimation exponentially. This correction is applied to counteract the tendencies of these estimations to be biased towards zero at the start of training, providing a more accurate estimation of the gradients.  $\epsilon$  acts as a safeguard against numerical errors, allowing the Adam optimizer to adjust the learning rates adaptively for each parameter without risk of being divided by zero errors.

#### 4.2. Performance Evaluation Metrics for Supply and Demand Forecasting

Evaluating the performance of the proposed framework involves calculating various metrics related to actual and predicted values of supply and demand (PV, wind, and load), such as MAE and RMSE [23]. We define  $z' = [PV_{\text{pred}}, W_{\text{pred}}, L_{\text{pred}}]$  and  $z = [PV_{\text{act}}, W_{\text{act}}, L_{\text{act}}]$ , where  $PV_{\text{pred}}$ ,  $PV_{\text{act}}$ ,  $W_{\text{pred}}$ ,  $W_{\text{act}}$ ,  $L_{\text{pred}}$ , and  $L_{\text{act}}$

represent the predicted and actual values for PV, wind, and load, respectively.  $z$  and  $z'$  represent vectors containing the actual and predicted values.  $MAE$  and  $RMSE$  are defined as

$$MAE = \frac{\sum_{t=1}^T |z_t - z'_t|}{T} \quad (8)$$

$$RMSE = \sqrt{\frac{\sum_{t=1}^T (z_t - z'_t)^2}{T}} \quad (9)$$

Forecasting bias ( $FB$ ) is used to measure the average tendency of predicted values in comparison to actual observed values, which is given by

$$FB = \frac{\sum_{t=1}^T (z_t - z'_t)}{T} \quad (10)$$

If  $FB$  is close to zero, it indicates that the predicted values are balanced with the actual observed values. A positive  $FB$  value indicates a tendency of the forecasting to overestimate the actual values, while a negative  $FB$  value indicates a tendency to underestimate the actual values.

### 5. Second-Stage Real-Time Optimal Energy Sharing Strategy

In this section, as the second stage, we propose an optimal real-time energy sharing model to maximize the utilization of PV and wind generation and minimize energy purchase and energy wastage. It considers the actual and forecasted availability of PV, wind, load demand, and ES capacity. Based on the first-stage predicted values, we assume the GICNs act as energy prosumers (both energy providers and buyers) through the bidirectional energy sharing as shown in the second stage in Figure 1. The energy provider GICNs are assumed willing to share energy with others to utilize the unutilized PV, wind, and available idle ES energy, while the energy buyers obtain energy from neighboring GICNs or ADN [22]. Ensure that the energy surplus is non-negative, indicating that the supply either meets or exceeds demand. When supply exceeds demand, there is extra energy available for sharing. If the energy surplus is negative, it indicates a supply and demand imbalance. In these cases, some GICNs may have insufficient PV and wind energy to meet their load demands, while others may have unutilized PV and wind energy. To address this issue, an optimal energy sharing strategy among GICNs is proposed.

Based on the first-stage system model, the total actual and predicted PV and wind generation are formulated as

$$P_{\text{pred}}(t) = PV_{\text{pred}}(t) + W_{\text{pred}}(t) \quad (11)$$

$$P_{\text{act}}(t) = PV_{\text{act}}(t) + W_{\text{act}}(t) \quad (12)$$

where  $P_{\text{pred}}$  and  $P_{\text{act}}$  are the total predicted and actual values of PV and wind generation, respectively. As energy providers mode, the GICNs have surplus energy from PV, wind, and ES, and can participate in the DR to maximize surplus energy utilization and minimize energy wastage. As energy buyer mode GICNs, when the PV, wind generation, and stored energy in ES is not enough to meet their load demand, the additional energy will be brought from the other GICNs or ADN to fill the energy gaps [12].

The predicted and actual surplus energy denoted by  $S_{\text{pred}}(t)$  and  $S_{\text{act}}(t)$  at time step  $t$  are considered by subtracting the total predicted and actual load demand from the total predicted and actual energy generation to find the available surplus energy provider and buyer mode (PM and BM), which are formulated as

$$S_{\text{pred}}(t) = \begin{cases} \min(P_{\text{pred}}(t) - L_{\text{pred}}(t), S_{\text{pred,max}}) & \text{PM} \\ \max(P_{\text{pred}}(t) - L_{\text{pred}}(t), -S_{\text{pred,max}}) & \text{BM} \end{cases} \quad (13)$$

$$S_{\text{act}}(t) = \begin{cases} \min(P_{\text{act}}(t) - L_{\text{act}}(t), S_{\text{act,max}}) & \text{PM} \\ \max(P_{\text{act}}(t) - L_{\text{act}}(t), -S_{\text{act,max}}) & \text{BM} \end{cases} \quad (14)$$

where  $S_{\text{pred,max}}$  and  $S_{\text{act,max}}$  are the predicted and actual maximum surplus energy.

For each GICN that has an ES system, the amount of energy that is discharged from ES is primarily to meet their own energy shortfall or to share with others during a specific time step  $t$ , which is formulated as

$$E_{\text{dis}}(t) = \begin{cases} E_{\text{dis,max}} & \text{PM} \\ \min(L_{\text{pred/act}}(t) - P_{\text{pred/act}}(t), E_{\text{dis,max}}) & \text{BM} \end{cases} \quad (15)$$

where  $E_{\text{dis}}(t)$  and  $E_{\text{dis,max}}$  represent the amount of discharge and maximum discharge energy from ES. As an energy PM, the ES discharging condition for each GICN is defined by the available maximum ES energy, which is potentially discharged to share with others. It typically occurs when there is surplus energy beyond the local demand. As an energy BM, the ES discharging condition is primarily to fill their own energy shortfall, which occurs when generation from PV and wind is insufficient. The constraint for the amount of energy currently stored in the ES after discharging is limited based on the capacity of ES, which is given by  $E_{\text{min}} \leq E(t) \leq E_{\text{max}}$ .  $E_{\text{min}}$  and  $E_{\text{max}}$  are the minimum and maximum capacity of ES (kWh), and  $E(t)$  is the remaining available energy of ES at time step  $t$ . Considering the predicted and actual surplus energy and the available discharge energy stored in ES, the predicted and actual shared energy for each GICN are defined as

$$X_{\text{pred}}(t) = S_{\text{pred}}(t) + E_{\text{dis}}(t) \quad (16)$$

$$X_{\text{act}}(t) = S_{\text{act}}(t) + E_{\text{dis}}(t) \quad (17)$$

where  $X_{\text{pred}}(t)$  and  $X_{\text{act}}(t)$  represent the predicted and actual shared energy at time step  $t$ . For the shared energy decision variables of the optimization model, if  $X_{\text{act}}(t), X_{\text{pred}}(t) > 0$ , it means the GICNs are in PM, and if  $X_{\text{act}}(t), X_{\text{pred}}(t) \leq 0$ , it means the GICNs are in BM. The shared energy should satisfy the constraints that  $\sum_t (X_{\text{pred}}(t), X_{\text{act}}(t)) = 0$ , which represents the sum of all shared energy across all time steps should equal zero. It implies balanced energy transactions over the period leading to no net energy accumulation or deficit. In addition, the shared energy should satisfy the constraints that  $0 \leq |X_{\text{pred}}(t), X_{\text{act}}(t)| \leq (X_{\text{pred,max}}(t), X_{\text{act,max}}(t))$ , where  $X_{\text{pred/act,max}}$  is the maximum shared energy. Considering the predicted and actual values of PV, wind, load demand, and the available discharge energy in ES, the predicted and actual brought energy are given by

$$G_{\text{pred}}(t) = \max(L_{\text{pred}}(t) - P_{\text{pred}}(t) - E_{\text{dis}}(t), 0) \quad (18)$$

$$G_{\text{act}}(t) = \max(L_{\text{act}}(t) - P_{\text{act}}(t) - E_{\text{dis}}(t), 0) \quad (19)$$

In this case, there is a constraint for energy BM GICNs, which is

$$-G_{\text{pred}}(t) \leq X_{\text{pred}}(t) \leq 0, -G_{\text{act}}(t) \leq X_{\text{act}}(t) \leq 0 \quad (20)$$

The operational constraints in (20) ensure that GICNs in BM can only buy energy to fill their deficits, but cannot provide energy. The shared energy is limited to a maximum of zero, indicating no energy is shared outwardly, and a minimum is set by their energy shortfall, meaning they can only buy energy from neighboring GICNs or ADN to meet their energy needs. Based on the energy interaction of PM and BM of GICNs, the current amount of energy stored in the ES system is updated as

$$\begin{cases} E(t+1) = E(t) + (S_{\text{pred/act}}(t)) - (X_{\text{pred/act}}(t)), & \text{PM} \\ E(t+1) = E(t) - E_{\text{dis}}(t), & \text{BM} \end{cases} \quad (21)$$

### 5.1. Objective Problem Formulation

The key purpose of the optimal energy sharing is to maximize the utilization of wind and PV generation, while simultaneously minimizing costs of energy purchase and wastage. For this, we apply a mixed-integer linear programming (MILP) approach to effectively handle both the discrete and continuous aspects of the optimization



problem. The predicted and actual total power generation utilization  $U_{\text{pred}}(t)$  and  $U_{\text{act}}(t)$  which are effectively utilized by the GICNs [8] are calculated as

$$\begin{aligned} U_{\text{pred}}(t) &= \min(P_{\text{pred}}(t), L_{\text{pred}}(t)) + \max(0, X_{\text{pred}}(t)) \\ U_{\text{act}}(t) &= \min(P_{\text{act}}(t), L_{\text{act}}(t)) + \max(0, X_{\text{act}}(t)) \end{aligned} \quad (22)$$

where  $\min(P_{\text{pred/act}}(t), L_{\text{pred/act}}(t))$  represents the self-supplied load demand that is directly supplied by the self-produced PV and wind generation. In (22), the problem aims to maximize the utilization of renewable energy sources by sharing surplus energy and reducing energy wastage among GICNs. To solve this maximization problem, we employ the MILP approach. MILP is particularly suitable here because it allows for the integration of discrete decision-making with continuous operational adjustments, which is essential in managing energy distribution systems where both types of decisions are critical. The optimization problem of maximizing total power generation utilization is formulated as

$$\begin{aligned} &\text{maximize } U_{\text{pred/act}}(t) \\ &\text{s.t. } 0 \leq X_{\text{pred/act}} \leq (S_{\text{pred/act}}(t) + E_{\text{dis}}(t)), \\ &E_{\text{min}} \leq E_{\text{dis}}(t) \leq E_{\text{max}} \end{aligned} \quad (23)$$

An additional critical objective is to reduce the costs associated with purchasing additional energy. By implementing energy sharing, maximizing renewable energy generation, and efficiently using stored energy, the model aims to decrease the need for external energy purchases, leading to cost savings for all participants in the network. The net energy cost is formulated as the energy bought from the neighboring GICN or from ADN minus the amount of sold energy at time step  $t$ . By using the MILP algorithm, the optimization problem of minimizing the net cost of energy ( $C_{\text{net}}$ ) is formulated as

$$\begin{aligned} C_{\text{net}} &= \text{minimize } \sum_{t=1}^T (\gamma G_{\text{pred/act}}(t) - \delta X_{\text{pred/act}}(t)) \\ &\text{s.t. } P_{\text{pred/act}}(t) + E_{\text{dis}}(t) + G_{\text{pred/act}}(t) = L_{\text{pred/act}}(t), \\ &0 \leq G_{\text{pred/act}} \leq (L_{\text{pred/act}}(t) - P_{\text{pred/act}}(t) - E_{\text{dis}}(t)), \\ &0 \leq X_{\text{pred/act}} \leq (S_{\text{pred/act}}(t) + E_{\text{dis}}(t)), \\ &E_{\text{min}} \leq E_{\text{dis}}(t) \leq E_{\text{max}} \end{aligned} \quad (24)$$

where  $\gamma$  and  $\delta$  are the costs associated with energy bought and sold, respectively.

### 5.2. Performance Metric Evaluation for Energy Sharing Efficiency

The self-sufficiency ratio (SSR) is a metric used to evaluate the degree to which a GICN can meet its energy demand with its own renewable energy generation, which is given by

$$SSR_{\text{pred/act}}(t) = \sum_t \left( \frac{P_{\text{pred/act}}(t) - L_{\text{pred/act}}(t) + E_{\text{dis}}(t)}{L_{\text{pred/act}}(t)} \right) \quad (25)$$

Performance metric evaluation for energy sharing efficiency refers to the evaluation of the effectiveness of energy sharing strategies within a system in achieving their intended goals. The self-consumption rate (SCR) is a metric that quantifies the proportion of local wind and PV generation directly consumed by GICNs. The formula for SCR is given by

$$SCR_{\text{pred/act}} = \sum_t \left( \frac{L_{\text{pred/act}}(t) - P_{\text{pred/act}}(t)}{P_{\text{pred/act}}(t)} \right) \quad (26)$$

## 6. Results and Discussions

### 6.1. Basic Data

This section focuses on validating the numerical performance of the proposed CNN-LSTM model for supply and demand forecasting, as well as the bidirectional real-time energy sharing strategies through simulations. The

real-time power supply and load demand data for GICN users is obtained from the live data portal of a central repository for the collection and publication of electricity generation for the pan-European market at <https://transparency.entsoe.eu/dashboard/show>. We use time series data recorded at 15-min intervals for 8 days (22 January 2024 to 29 January 2024) for our simulation, executed in Python using PyTorch ML library, which is trained, validated, and tested on 70%, 15%, and 15% of the dataset, respectively. The costs associated with energy bought and sold are  $\gamma = 0.35\$/\text{kWh}$  and  $\delta = 0.5\$/\text{kWh}$ . The components, descriptions, and associated hyperparameters of the hybrid CNN-LSTM model are discussed. The hyperparameters of the hybrid CNN-LSTM models are set for the training process, and the model component parameters and their descriptions are outlined in Table 1. Table 2 shows the parameters set for ES Type.

**Table 1.** Model Components, Descriptions, and Hyperparameters.

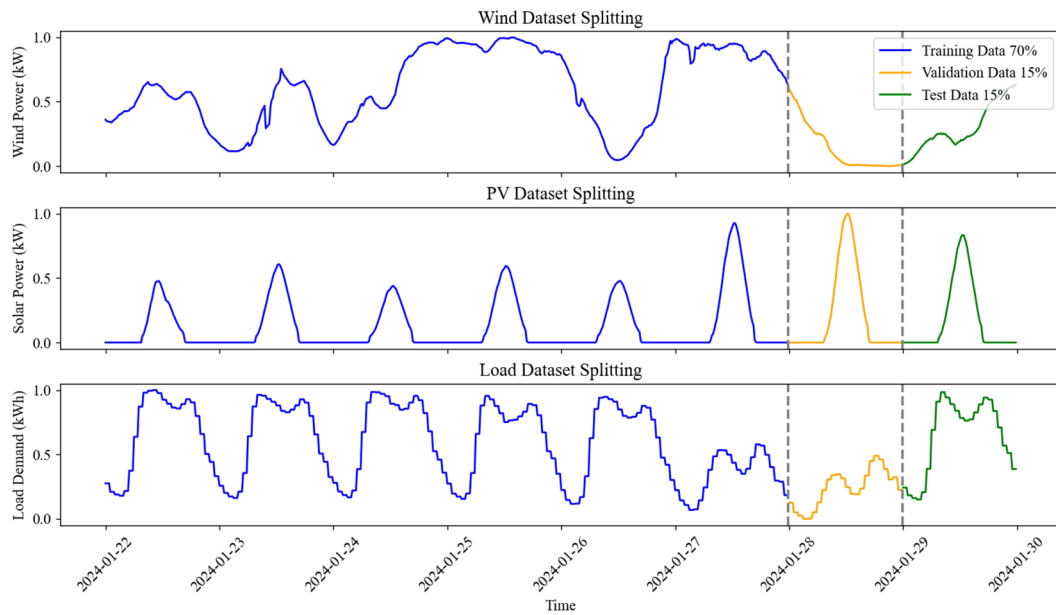
Components	Description	Hyperparameters
Data Preprocessing	Feature creation and data scaling	MinMaxScaler
CNN Layer (conv1)	A convolutional layer that processes the input features using kernels.	Input channels = number of features, output channels = 64, kernel size = 1
Activation (ReLU)	A non-linear activation function that applied after the convolutional layer to introduce non-linearity.	$f(x) = \max(0, x)$
LSTM Layer	An LSTM layer that processes sequences of data, capturing long-term dependencies.	Input size = 64 (matches the output of conv1), hidden size = 100
DataLoaders	Utilities to batch, shuffle, and load the data efficiently during training and evaluation.	Batch size = 128
Activation	Activation functions in LSTM Layers	Tanh (-1, 1) and sigmoid (0, 1)
Model Instantiation	Creating instances of the CNN-LSTM model with specified configurations for different datasets.	Number features = 1, hidden size = 100
Loss Function	The criterion used to evaluate the difference between the predicted outputs and actual targets.	MSELoss
Optimizer	The optimization algorithm used to adjust model parameters via backpropagation.	Adam, learning rate (lr = 0.001)
Training Loop	The process of training the model through forward and backward passes, adjusting the model with each batch of data.	Number epochs = 100

**Table 2.** Parameters Set for ES Type.

Parameters	Value
Maximum capacity (kWh)	20
Maximum discharge rate (kW)	10
Minimum limit (kWh)	0.2

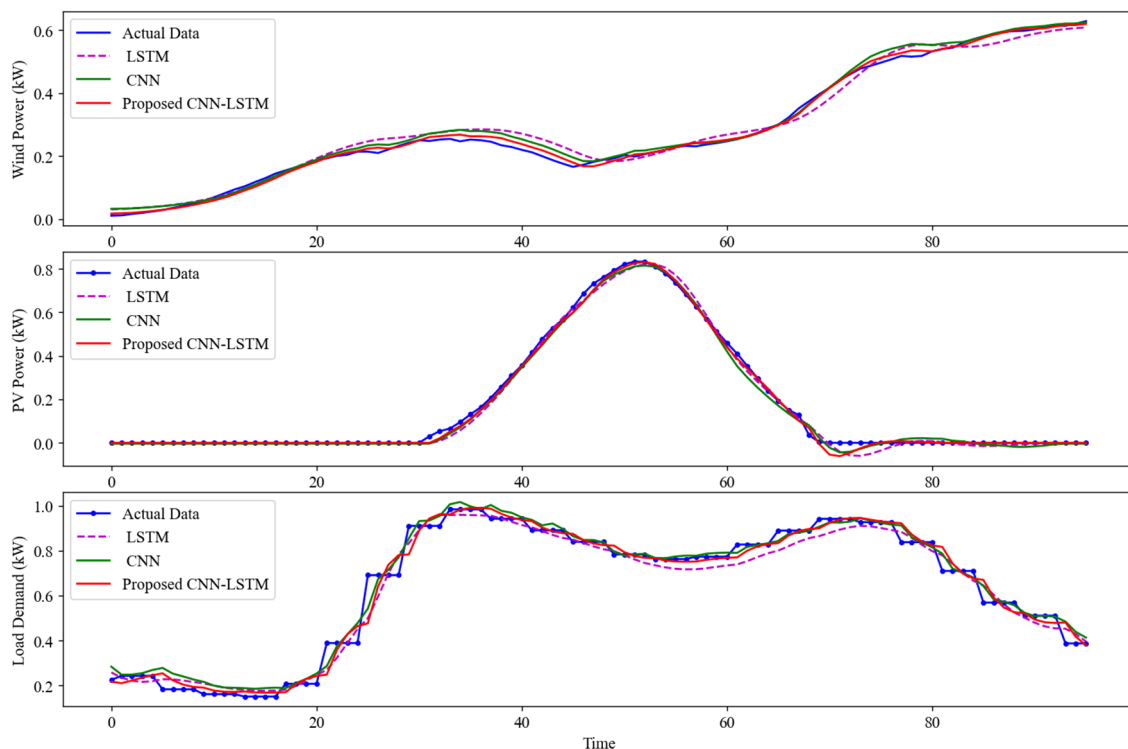
### 6.2. First-Stage Supply and Load Demand Forecasting Analysis

Figure 3 illustrates the process of splitting the time-series data of wind and PV generation, as well as load, into training, validation, and testing datasets. This key step in model development ensures that models not only fit the dataset used to train the model but also perform effectively to new and unseen data to provide consistent predictions.



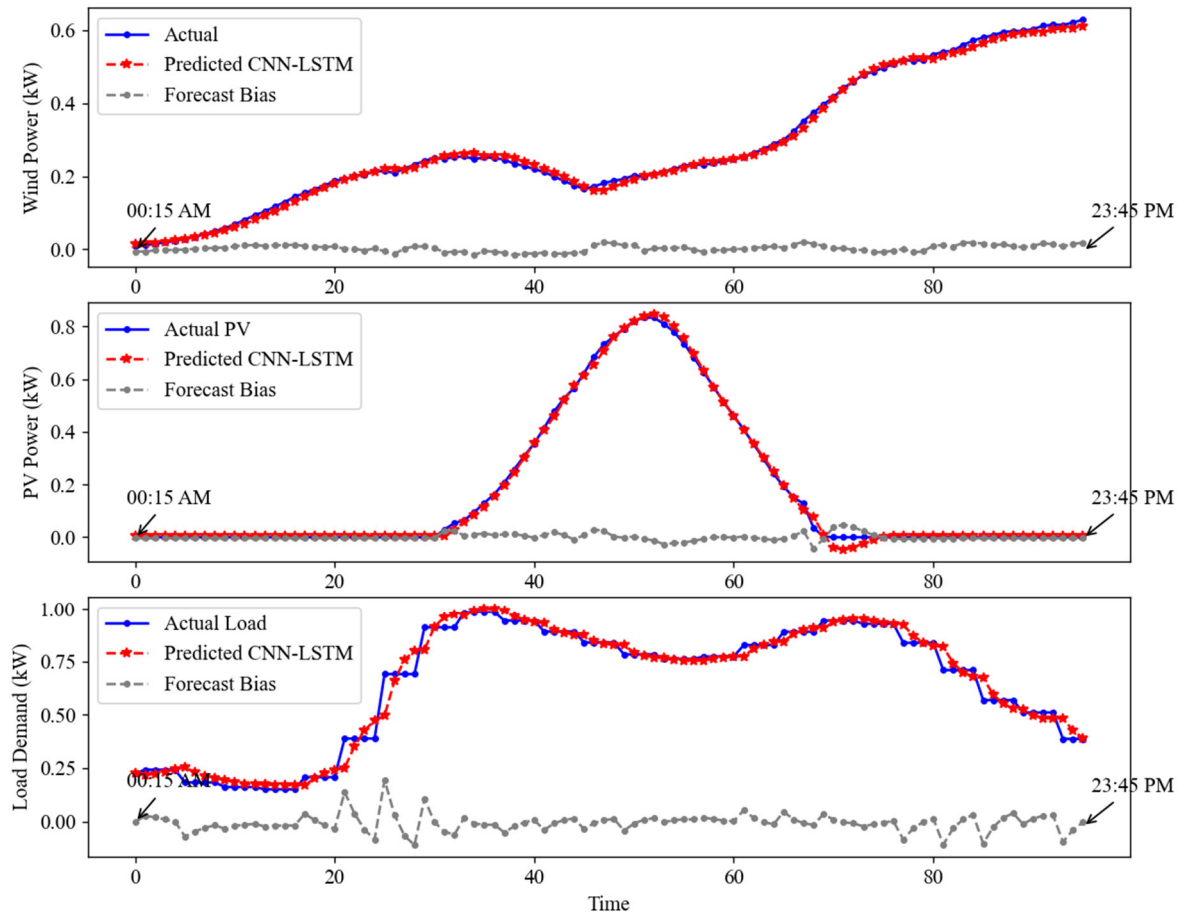
**Figure 3.** PV, wind, and load dataset splitting for training, validation, and testing.

Figure 4 compares the last 24 h of predictions, recorded at 15-min intervals, from the LSTM, CNN, and hybrid CNN-LSTM models. The hybrid CNN-LSTM model demonstrates superior accuracy in forecasting time-series data compared to the single models (LSTM and CNN). The LSTM model captures general trends but exhibits higher fluctuations and deviations during rapid changes. The CNN model handles short-term fluctuations well but struggles with longer-term patterns. In contrast, the hybrid CNN-LSTM model closely follows the actual data for wind power, PV generation, and load demand, effectively reducing forecasting errors. It captures both spatial and temporal dynamics, providing smoother and more accurate predictions. Overall, the hybrid CNN-LSTM model consistently outperforms the single models in terms of forecasting accuracy, making it more effective in understanding and forecasting the dynamics of renewable energy generation and load demand. The enhanced accuracy is crucial for reliable and efficient energy supply management.



**Figure 4.** Comparison of LSTM, CNN, and hybrid CNN-LSTM model for predictions.

Figure 5 shows the predicted values compared to the actual observed values at 15-min intervals for the last 24 h, generated by the proposed hybrid CNN-LSTM model incorporating a FB improvement. The incorporation of the FB error metric significantly improves the model’s performance. The error values approaches zero, indicating the model’s effectiveness and accuracy in forecasting.



**Figure 5.** The last 24-h 15-min increments data point prediction for proposed CNN-LSTM with FB.

### 6.3. Forecasting Performance Metrics

Based on the supply and demand forecasting, the performance metrics (MAE and RMSE) of the LSTM, CNN, and the proposed hybrid CNN-LSTM models for the wind, PV, and load datasets are compared as shown in Table 3. The hybrid CNN-LSTM model demonstrates higher forecasting accuracy for all datasets. This hybrid approach effectively leverages the strengths of both CNN (for local feature extraction) and LSTMs (for learning long-term dependencies), resulting in significant performance improvements.

**Table 3.** Performance metrics of LSTM, CNN, and Hybrid CNN-LSTM models.

Metric	LSTM			CNN			Hybrid CNN-LSTM		
	Wind	PV	Load	Wind	PV	Load	Wind	PV	Load
MAE	0.021	0.018	0.035	0.264	0.163	0.646	0.007	0.008	0.012
RMSE	0.025	0.023	0.046	0.336	0.273	0.715	0.009	0.001	0.044

### 6.4. Second-Stage Bidirectional Real-Time Energy Sharing Analysis

Figure 6 presents the second-stage bidirectional real-time energy sharing strategies. This simulation captures the interaction among total energy generation, load demand, surplus energy, ES discharging, and imported energy throughout the final observation day. Particularly, energy sharing is increased during periods when total generation surpasses load demand and the presence of surplus energy in ES. Positive values in the bar plot represent imported energy when load surpasses total power generation under situations needing additional power to satisfy load demand. In these instances, surplus energy is depicted in a negative direction, stressing the GICN’s imperative to fill the energy shortage. ES is presumed to be discharged to address this gap when no surplus is available or can

alternatively be discharged to share energy with other GICNs that have no surplus energy. Positive surplus, on the other hand, denotes scenarios where generation outmatches demand, availing surplus for sharing. This analytical representation emphasizes the pivotal role of real-time energy sharing strategies in encouraging the sustainability and operational efficacy of grid-integrated community networks.

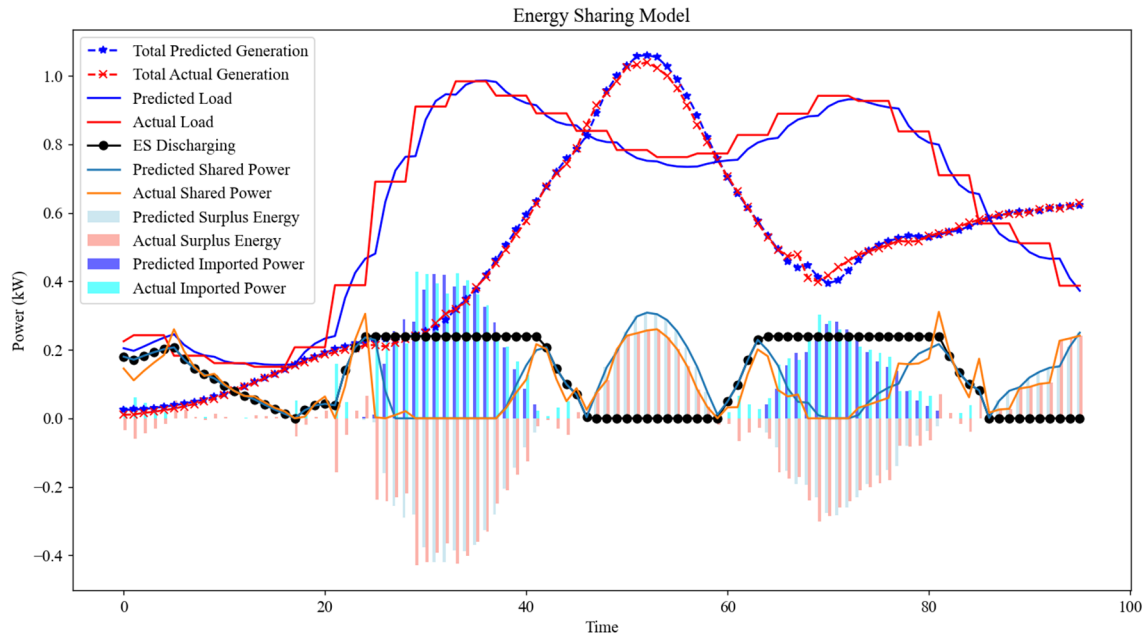


**Figure 6.** Second-stage real-time energy sharing based on predicted supply and load model.

Figure 7 provides a visual representation comparing the effectiveness of total power generation utilization in scenarios with and without the implementation of an energy sharing strategies across different time slots. With implemented energy sharing, both predicted and actual generation utilization rates are generally higher, illustrating the efficiency and effectiveness with which the generated energy is utilized. Conversely, the absence of energy sharing leads to a noticeable decline in utilization, underscoring potential inefficiencies and the risk of increased energy wastage. This simulation analysis stresses the important role of energy sharing in improving the sustainability and efficiency of renewable energy systems.

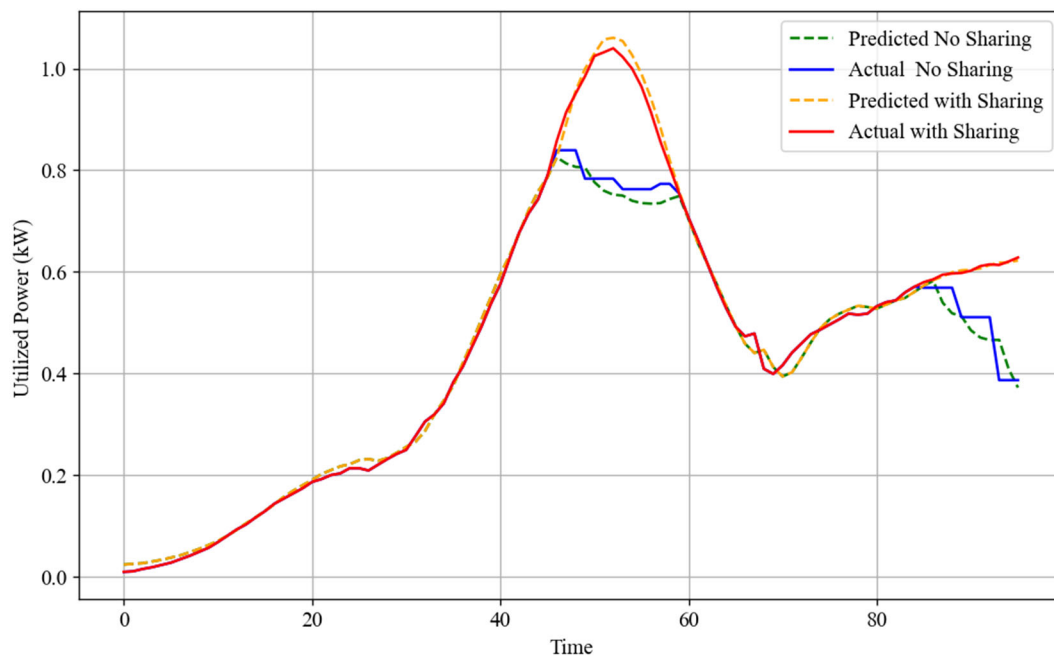


**Figure 7.** Total generation utilization effectiveness with and without energy sharing.

Figure 8 shows the performance of the SSR and SCR within GICNs. These metrics are involved in evaluating the effectiveness of GICNs in managing and utilizing their energy production. SSR reflects the degree to which GICNs can fulfill their energy needs independently, while SCR evaluates the proportion of self-generated energy that is consumed within GICNs. High SSR and SCR values are indicative of efficient energy production and consumption practices, stressing the GICNs' capability to maximize the utility of their renewable energy sources and reduce reliance on external power supplies.

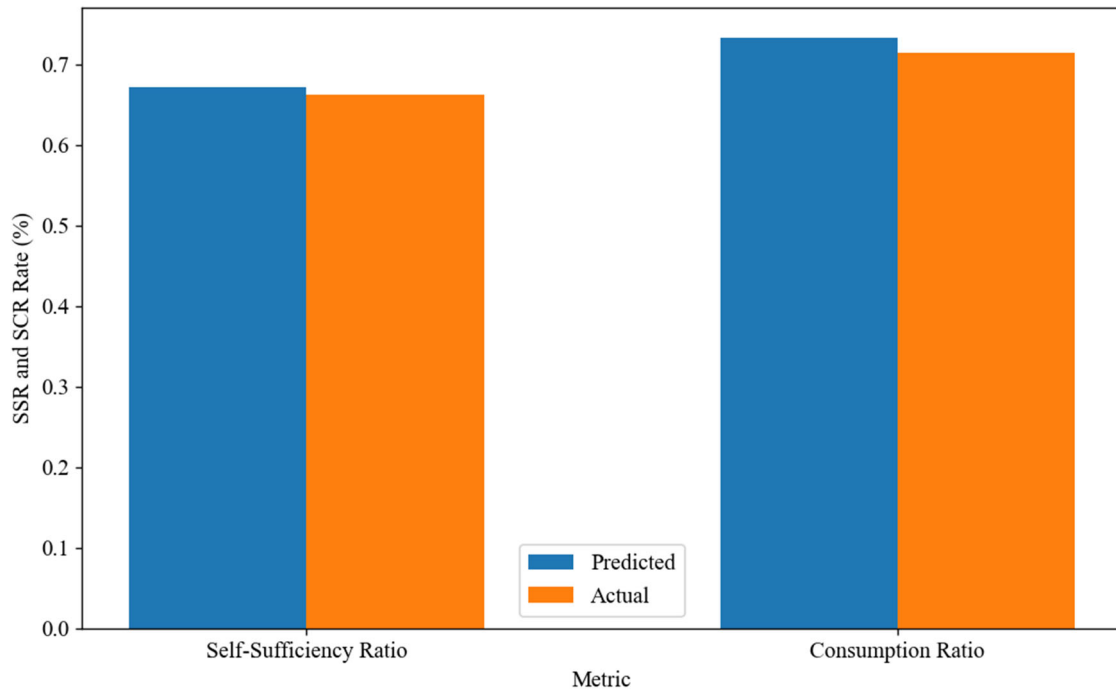


Figure 8. SSR and SCR performance metrics for GICNs.

Figure 9 provides a comprehensive overview of the dynamics of energy transactions between energy sold, energy bought, and the net energy costs over time. A dynamic increase in energy sold correlates with instances of generation exceeding load demand. Conversely, energy purchases, depicted through negative values, emerge when demand surpasses the total generation, necessitating external procurement. A negative net energy cost implies that the revenue from energy sold exceeds the cost of energy that the GICN purchased from neighboring GICNs or AND, indicating a degree of energy independence, where a GICN relies less on external energy supplies. Conversely, a positive net energy cost means that the cost of energy bought surpasses the revenue from selling energy, leading to a net expense within GICNs.

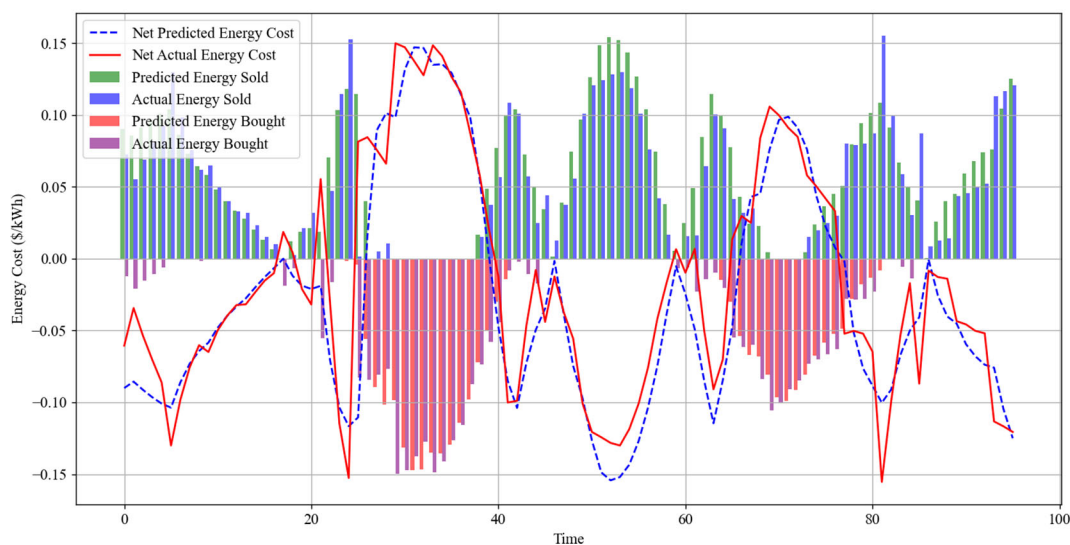


Figure 9. Energy sold, bought, and net energy costs.

## 7. Conclusion

This study proposed a comprehensive exploration of the integration and efficacy of a hybrid CNN-LSTM model for forecasting supply and demand in energy systems, complemented by an innovative bidirectional real-time energy sharing framework within GICNs. Through rigorous simulations, we demonstrated the superior accuracy of the proposed hybrid model over a single LSTM and CNN models in forecasting wind, PV, and load demand. Our first-stage model analysis stressed the importance of splitting time-series data into training, validation, and testing sets to ensure that the model not only fits well with the historical data but also generalizes effectively to new and unseen data. The results from this stage revealed that the hybrid CNN-LSTM model is adept at capturing both the spatial and temporal dimensions of the dataset, significantly enhancing forecasting accuracy. In the second-stage analysis, we delved into the dynamics of real-time energy sharing, illustrating how energy sharing strategies could dynamically respond to fluctuations in energy generation and demand. The findings highlighted the potential of energy sharing strategies to mitigate gaps between energy supply and demand, thereby enhancing the sustainability and efficiency of GICNs. Notably, the implementation of energy sharing was shown to optimize the utilization of generated energy and reduce wastage and costs. Simulation experiments and performance evaluations are conducted to validate the forecasting model and the real-time energy-sharing strategy. In conclusion, the integration of the hybrid CNN-LSTM forecasting model with bidirectional real-time energy-sharing strategies represents an important advancement in the field of smart GICN energy management. Building on this study, future research could explore advanced neural network architectures to improve energy forecasting considering feature selection and seasonal trends, and investigate energy sharing mechanisms for decentralized energy systems to enhance grid security and efficiency in GICNs.

**Author Contributions:** A.G.J.: Conceptualization, Methodology, Software, Writing—Original Draft Preparation; R.B.: Data Curation, Writing—Original Draft Preparation; Z.Y.: Visualization, Investigation; Z.W.: Supervision; Z.Z. and X.W.: Validation, Writing—Reviewing and Editing. All authors have read and agreed to the published version of the manuscript.

**Funding:** This work is supported by Science and Technology Project of China Southern Power Grid Company Limited under Grant Number 1500002023030103JL00320.

**Institutional Review Board Statement:** Not applicable.

**Informed Consent Statement:** Not applicable.

**Data Availability Statement:** Not applicable.

**Acknowledgments:** The authors would like to thank the Key Laboratory of Alternate Electrical Power System with Renewable Energy Sources at North China Electric Power University, for its support of this paper.

**Conflicts of Interest:** All authors declare no conflict of interest.

## References

1. Blesslin, S.T.; Wessley GJ, J.; Kanagaraj, V.; Kamatchi, S.; Radhika, A.; Janeera, D.A. Microgrid Optimization and Integration of Renewable Energy Resources: Innovation, Challenges and Prospects. *Integr. Renew. Energy Sources Smart Grid* **2021**, *2021*, 239–262.
2. Liao, H.; Zhou, Z.; Jia, Z.; Shu, Y.; Tariq, M.; Rodriguez, J.; Frascolla, V. Ultra-Low AoI Digital Twin-Assisted Resource Allocation for Multi-Mode Power IoT in Distribution Grid Energy Management. *IEEE J. Sel. Areas Commun.* **2023**, *41*, 3122–3132.
3. Kabeyi, M.J.B.; Olanrewaju, O.A. Smart grid technologies and application in the sustainable energy transition: A review. *Int. J. Sustain. Energy* **2023**, *42*, 685–758.
4. Akinte, O.O.; Prasartkaew, B. Grid Integrated Renewable Energy Network in Variety Sources. In Proceedings of the 2023 International Conference on Power, Energy and Innovations (ICPEI), Phraчуап Khirikhan, Thailand, 18–20 October 2023; pp. 46–51.
5. Zhou, Z.; Dong, M.; Ota, K. Secure and Efficient Vehicle-to-Grid Energy Trading in Cyber Physical Systems: Integration of Blockchain and Edge Computing. *IEEE Trans. Syst. Man Cybern. Syst.* **2020**, *50*, 43–57.
6. Maheswari, K.L.; Sathya, B.; Jeylani AM, A. Mitigating Measures to Address Challenges of Renewable Integration—Forecasting, Scheduling, Dispatch, Balancing, Monitoring, and Control. *Integr. Renew. Energy Sources Smart Grid* **2021**, *2021*, 281–304.
7. Li, P.; Wang, J.; Zhang, C.; Wang, N.; Dou, Z.; Zhou, X.; Wang, G. Day-ahead Time-sharing Optimal Scheduling for Community Integrated Energy System Based on Multi-energy Time-series Analysis. In Proceedings of the 2022 IEEE/IAS Industrial and Commercial Power System Asia (I&CPS Asia), Shanghai, China, 8–11 July 2022; pp. 738–743.

8. Liao, H.; Zhou, Z.; Liu, N.; Zhang, Y.; Xu, G.; Wang, Z.; Mumtaz, S. Cloud-Edge-Device Collaborative Reliable and Communication-Efficient Digital Twin for Low-Carbon Electrical Equipment Management. *Trans. Ind. Inform.* **2023**, *19*, 1715–1724.
9. Han, M.E.; Alston, M.; Gillott, M. A multi-vector community energy system integrating a heating network, electricity grid and PV production to manage an electrified community. *Energy Build.* **2022**, *266*, 112105.
10. Minuto, F.D.; Lanzini, A. Energy-sharing mechanisms for energy community members under different asset ownership schemes and user demand profiles. *Renew. Sustain. Energy Rev.* **2022**, *168*, 112859.
11. Zhou, Z.; Jia, Z.; Liao, H.; Lu, W.; Mumtaz, S.; Guizani, M.; Tariq, M. Secure and Latency-Aware Digital Twin Assisted Resource Scheduling for 5G Edge Computing-Empowered Distribution Grids. *IEEE Trans. Ind. Inform.* **2022**, *18*, 4933–4943.
12. Liu, N.; Yu, X.; Fan, W.; Hu, C.; Rui, T.; Chen, Q.; Zhang, J. Online Energy Sharing for Nanogrid Clusters: A Lyapunov Optimization Approach. *IEEE Trans. Smart Grid* **2017**, *9*, 4624–4636.
13. Ayoub, N.; Musharavati, F.; Pokharel, S.; Gabbar, H.A. ANN Model for Energy Demand and Supply Forecasting in a Hybrid Energy Supply System. In Proceedings of the 2018 IEEE International Conference on Smart Energy Grid Engineering (SEGE), Oshawa, ON, Canada, 12–15 August 2018; pp. 25–30.
14. Golder, A.; Jneid, J.; Zhao, J.; Bouffard, F. Machine Learning-Based Demand and PV Power Forecasts. In Proceedings of the 2019 IEEE Electrical Power and Energy Conference (EPEC), Montreal, QC, Canada, 16–18 October 2019; pp. 1–6.
15. Zhang, X.; Wang, Z.; Liao, H.; Zhou, Z.; Ma, X.; Yin, X.; Lv, G. Optimal capacity planning and operation of shared energy storage system for large-scale photovoltaic integrated 5G base stations. *Int. J. Electr. Power Energy Syst.* **2023**, *147*, 108816.
16. Dimitropoulos, N.; Sofias, N.; Kapsalis, P.; Mylona, Z.; Marinakis, V.; Primo, N.; Doukas, H. Forecasting of short-term PV production in energy communities through Machine Learning and Deep Learning algorithms. In Proceedings of the 2021 12th International Conference on Information, Intelligence, Systems and Applications (IISA), Chania Crete, Greece, 12–14 July 2021; pp. 1–6.
17. Wen, L.; Zhou, K.; Yang, S.; Lu, X. Optimal load dispatch of community microgrid with deep learning based solar power and load forecasting. *Energy* **2019**, *171*, 1053–1065.
18. Qayyum, F.; Jamil, H.; Jamil, F.; Kim, D. Predictive Optimization Based Energy Cost Minimization and Energy Sharing Mechanism for Peer-to-Peer Nanogrid Network. *IEEE Access* **2022**, *10*, 23593–23604.
19. Wang, K.; Qi, X.; Liu, H. Photovoltaic power forecasting based LSTM-Convolutional Network. *Energy* **2019**, *189*, 116225.
20. Zhang, X.; Wang, Z.; Zhou, Z.; Liao, H.; Ma, X.; Yin, X.; Liu, Y. Optimal Dispatch of Multiple Photovoltaic Integrated 5G Base Stations for Active Distribution Network Demand Response. *Front. Energy Res.* **2022**, *10*, 919197.
21. Shi, M.; Xu, K.; Wang, J.; Yin, R.; Wang, T.; Yong, T. Short-Term Photovoltaic Power Forecast Based on Long Short-Term Memory Network. In Proceedings of the 2019 IEEE 3rd International Electrical and Energy Conference (CIEEC), Beijing, China, 7–9 September 2019; pp. 2110–2116.
22. Mejdj, L.; Kardous, F.; Grayaa, K. Experimental Validation of PV Power Prediction with ML Models for Improved Grid Integration. In Proceedings of the 2023 20th International Multi-Conference on Systems, Signals and Devices (SSD), Mahdia, Tunisia, 20–23 February 2023; pp. 439–445.
23. Zhang, X.; Chau, T.K.; Chow, Y.H.; Fernando, T.; Iu, H.H., C. A Novel Sequence to Sequence Data Modelling Based CNN-LSTM Algorithm for Three Years Ahead Monthly Peak Load Forecasting. *IEEE Trans. Power Syst.* **2024**, *39*, 1932–1947.